MATHEMATICAL MODELING AND COMPUTING, Vol. 10, No. 4, pp. 1239–1249 (2023)

Numerically investigating the effects of slip and thermal convective on nanofluid boundary layer past a stretching/shrinking surface

Najib N.[1], Bachok N.[2,3], Rasedee A. F. N.[1], Salleh S. N. A.[4], Suhaimi W. N. W.[1]

[1] *Faculty of Economics and Muamalat, University Sains Islam Malaysia, Bandar Baru Nilai, 71800 Nilai, Negeri Sembilan, Malaysia*
[2] *Institute of Mathematical Research and Department of Mathematics and Statistics, Faculty of Science, University Putra Malaysia, 43400 Serdang, Selangor, Malaysia*
[3] *College of Computing, Informatics and Mathematics, University Teknologi MARA Kedah, Merbok 08400, Kedah, Malaysia*

(Received 26 September 2023; Revised 21 November 2023; Accepted 22 November 2023)

The study is focusing on the steady boundary layer flow, heat and mass transfer passing through stretching/shrinking sheet immersed in nanofluid in the presence of the second order slip velocity and thermal convective at the boundary. The governing partial differential equations are converted into ordinary differential equations by applying the similarity variables before being solved computationally using bvp4c function in Matlab software. The results of skin friction, heat transfer as well as mass transfer coefficient on the governing parameter such as the first order slip parameter, the second order slip parameter, Biot number, Brownian motion parameter and thermopherosis parameter are shown graphically in the discussion. The dual solutions exist in all range of stretching and shrinking parameter. Therefore the stability analysis is performed and concluded that the first solution is stable and physically relevant while the second solution acts in opposite way.

Keywords: *stability analysis; stretching/shrinking sheet; nanofluid; dual solution; heat and mass transfer; second order slip; thermal convective.*

2010 MSC: 80A20 **DOI:** 10.23939/mmc2023.04.1239

1. Introduction

The study on the second order slip velocity at the boundary is getting attraction among researchers nowadays. The fact that viscous fluid is normally sticks to the boundary cannot be accepted sometimes because for some types of fluid namely particulate fluids and rarefied gas there may be a slip between the fluid and the boundary when immersed in it [1–5]. The applications on the second order slip velocity in industrial processes can be found in polymer solutions and oil industry which involved emulsions process.

The second order slip velocity was modeled by [6]. Fang et al. [7] and Fang and Aziz [8] are among the first researchers who used the proposed model by considering the shrinking and stretching sheet respectively, in the presence of mass suction. Then, Nandeppanavar et al. [9] studied the slip flow through stretching sheet in nonlinear Navier boundary conditions. Instead of consider the flow horizontally, [10] and [11] consider the slip slow on the permeable vertical plate. The effects of slip flow on nanofluid have been done by Alam et al. [12] using Boungiorno model [13]. Inspired by previous works, a lot of research has been performed on the effect of the second-order slip using various types of fluids and surfaces, see [14–20]. Recently, Bakar et al. [21] examined the impact of the second-order velocity slip, suction, and heat absorption on hybrid nanofluid flow in a porous medium. They noticed from their study that the participating parameters of suction, porous medium permeability, and nanoparticle volume fraction enhance the boundary layer thickness, while the second-order velocity slip parameter tends to decay the fluid flow. A numerical study has been done by Jauhri and Mishra [22] considering the MHD nanofluid flow in porous media over a stretchable surface with the second-order velocity slip.

The importance of the stability analysis is to verify which solution is in steady state and physically relevant. The method of analyzing the stability is by using the bvp4c code in Matlab software. Merkin [23] was the first who made the analysis to test the stability flow, followed by Weidman et al. [24] and Merill et al. [25], who used the method to find the stability of the solutions. The stability flow in steady and unsteady cases are respectively studied by Ishak [26] and Hafidzuddin et al. [27]. Nazar et al. [28] and Noor et al. [29, 30] studied the stability analysis on the different type of plate which are shrinking sheet and moving plate. Due to the significance of using the stability analysis in the flow, many authors took this advantage to perform more investigations considering various fluids and effects [31–35]. Recently, Rasool et al. [36] investigated the magnetohydrodynamics flow of copper-alumina water hybrid nanofluid under the influence of Joule heating and viscous dissipation past a porous shrunk surface. They found from their study that the first solution is stable, meanwhile, the second one is unstable.

Due to increased heat transfer performance, analyzing the boundary layer flow with a convective boundary condition has recently been a topic of substantial investigation. Aziz [37] start the early experiment by studying a laminar thermal boundary layer flow near a flat plate with a convective boundary condition. Noghrehabadi et al. [38] studied the boundary layer flow and heat transfer past a stretching surface by taking into account the effects of partial slip and a thermal convective boundary condition. In their study, Buongiorno model [13] is chosen in the simulation of the nanofluid since it has two notable effects namely Brownian movement and thermophoretic diffusion that enhance the thermal conductivity of ordinary fluids. Since then, many works have been carried out to study the convective boundary condition using Buongiorno nanofluid model [39–43].

Considering the research that has been discussed earlier, our focus is to study the effect of second-order velocity slip together with the thermal convective on the nanofluid flow past a stretching/shrinking surface by implementing the stability analysis. This idea has been adapted from the work of Noghrehabadi et al. [38]. The novelty of this work is to consider the same problem as Noghrehabadi et al. [38] but we have extended it to the stretching/shrinking surfaces and applied stability analysis to validate the obtained results. The outcomes of this study will be graphically shown, and the characteristics of the flow field will be discussed further. It is worth mentioning that no attempt has been made to such a present study.

2. Mathematical formulation

Consider the steady boundary-layer flow of a nanofluid past a stretching/shrinking plate as shown in Figure 1.

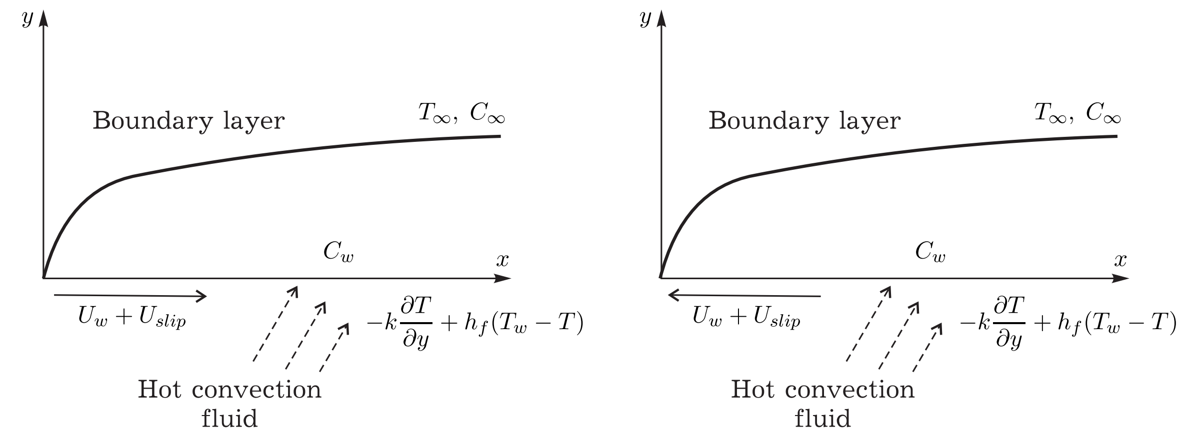

Fig. 1. Physical model for (a) stretching sheet and (b) shrinking sheet.

It is assumed that the velocity of the surface is $U_w = cx$ where c is a constant, and x is the coordinate component along the stretching/shrinking surface. The nanofluid flows takes place at $y = 0$, where y is the coordinate measured normal to the stretching/shrinking surface. Further, the velocity at the boundary is assumed to have a slip of order two (Wu [6]; Fang et al. [7]; Fang and Aziz [8])

$$\begin{aligned} U_{slip} &= \frac{2}{3}\left(\frac{3-\chi l^3}{\chi} - \frac{3}{2}\frac{1-l^2}{K_n}\right)\omega\frac{\partial u}{\partial y} - \frac{1}{4}\left(l^4 + \frac{2}{K_n^2}(1-l^2)\right)\omega^2\frac{\partial^2 u}{\partial y^2}, \\ &= A\frac{\partial u}{\partial y} + B\frac{\partial^2 u}{\partial y^2}, \end{aligned} \tag{1}$$

where A and B are constants, K_n is Knudsen number, $l = \min(l/K_n, 1)$, χ is the momentum accommodation coefficient with $0 \leqslant \chi \leqslant 1$, and ω is the molecular mean free path. Based on the definition of l, it is seen that for any given value of K_n, we have $0 \leqslant \chi \leqslant 1$. Since the molecular mean free path ω is always positive it results in that B is a negative number.

A flow with the convective heat transfer coefficient of h_f and temperature of T_f is flowing below the stretching/shrinking sheet. It is also assumed that at the stretching/shrinking surface, the temperature T and the nanoparticle fraction ϕ take constant values T_w and ϕ_w, respectively, while the values of T and ϕ in the ambient fluid (inviscid flow) are denoted by T_∞ and ϕ_∞, respectively. When y attends to infinity, the values of the temperature and nanoparticle fraction attend to the constant values of T_∞ and ϕ_∞ in the quiescent part of the nanofluid, respectively. ϕ and T indicate the fraction of nanoparticles and the temperature of flow, respectively. For nanofluids, by considering the dynamic effects of the nanoparticles and applying the boundary layer approximations the Buongiorno [13] convective transport equations in the Cartesian coordinate system of x and y can be written as follows [38,44,45]:

$$\frac{\partial u}{\partial x} + \frac{\partial v}{\partial y} = 0, \tag{2}$$

$$\frac{\partial u}{\partial t} + u\frac{\partial u}{\partial x} + v\frac{\partial u}{\partial y} = \nu\frac{\partial^2 u}{\partial y^2}, \tag{3}$$

$$\frac{\partial T}{\partial t} + u\frac{\partial T}{\partial x} + v\frac{\partial T}{\partial y} = \alpha\nabla^2 T + \Omega\left[D_B\frac{\partial \phi}{\partial y}\frac{\partial T}{\partial y} + \left(\frac{D_T}{T_\infty}\right)\left(\frac{\partial T}{\partial y}\right)^2\right], \tag{4}$$

$$\frac{\partial \phi}{\partial t} + u\frac{\partial \phi}{\partial x} + v\frac{\partial \phi}{\partial y} = D_B\frac{\partial^2 \phi}{\partial y^2} + \left(\frac{D_T}{T_\infty}\right)\frac{\partial^2 T}{\partial y^2}, \tag{5}$$

where u and v are the velocity components along the x and y axes, respectively, $a = k/(\rho c)_f$ is the thermal diffusivity of the fluid, ν is the kinematic viscosity coefficient and $\Omega = (\rho c)_p/(\rho c)_f$. The initial and boundary conditions of Eqs. (2)–(5) are taken to be

$$\begin{aligned} &t < 0\colon u = v = 0, \quad T = T_\infty, \quad \phi = \phi_\infty \quad \text{for any} \quad x, y, \\ &t \geqslant 0\colon u = \varepsilon U_w + U_{slip}, \quad v = v_w - k_f\left(\frac{\partial T}{\partial y}\right) = h_f(T_f - T), \quad D_B\frac{\partial \phi}{\partial y} + \frac{D_T}{T\ {}_\infty}\frac{\partial T}{\partial y} = 0 \quad y = 0, \\ &\qquad u \to 0, \quad T \to T_\infty, \quad \phi = \phi_\infty \quad \text{as} \quad y \to \infty, \end{aligned} \tag{6}$$

where $v = v_w$ is the constant mass flux velocity, D_B is the Brownian diffusion coefficient, D_T is the thermophoretic diffusion coefficient.

3. Steady state solution ($\partial/\partial t = 0$)

The mathematical analysis of the problem is simplified by introducing the following dimensionless variables

$$\psi = (c\nu)^{1/2} x f(\eta), \quad \eta = (c/\nu)^{1/2} y, \quad \theta(\eta) = \frac{T - T_\infty}{T_f - T_\infty}, \quad \beta(\eta) = \frac{\phi - \phi_\infty}{\phi_f - \phi_\infty}, \tag{7}$$

where ψ is the stream function defined as $u = \partial\psi/\partial y$ and $v = -\partial\psi/\partial x$ which identically satisfies Eq. (2). Substitute (7) into Eqs. (3)–(5), we obtain the following nonlinear ordinary differential equations

$$f''' + ff'' - f'^2 = 0, \tag{8}$$

$$\frac{1}{\mathrm{Pr}}\theta'' + f\theta' + \mathrm{Nb}\,\beta'\theta' + \mathrm{Nt}\,\theta'^2 = 0, \tag{9}$$

$$\beta'' + \mathrm{Le}\,f\beta' + \frac{\mathrm{Nt}}{\mathrm{Nb}}\theta'' = 0, \tag{10}$$

and the boundary conditions (6) become

$$\begin{gathered} f(0) = s, \quad f'(0) = \varepsilon + \sigma f''(0) + \delta f'''(0), \\ \theta'(0) = \mathrm{Bi}\,(\theta(0) - 1), \quad \mathrm{Nb}\,\beta'(0) + \mathrm{Nt}\,\theta'(0) = 0, \\ f'(\infty) \to 0, \quad \theta(\infty) \to 0, \quad \beta(\infty) \to 0, \end{gathered} \tag{11}$$

where $s = -\frac{v_w}{\sqrt{c\nu}}$ is mass suction parameter, Pr is the Prandt number, Le is Lewis number, Bi is the Biot number, Nb is the Brownian motion parameter, Nt is thermophoresis parameter, ε is the stretching/shrinking parameter, σ is the first-order velocity slip parameter and δ is the second-order velocity slip parameter defined as

$$\begin{gathered} \mathrm{Nb} = \frac{(\rho c)_p D_B(\phi_f - \phi_\infty)}{(\rho c)_f \nu}, \quad \mathrm{Nt} = \frac{(\rho c)_p D_T(T_f - T_\infty)}{(\rho c)_f \nu T_\infty}, \\ \mathrm{Pr} = \frac{\nu}{\alpha}, \quad \mathrm{Bi} = \frac{h_f}{k_f}\sqrt{\nu/c}, \quad \mathrm{Le} = \frac{\nu}{D_B}, \quad s = \frac{v_w}{\sqrt{\nu c}}, \quad \varepsilon = \frac{u}{U_w}, \end{gathered} \tag{12}$$

where $\varepsilon > 0$ corresponds to stretching sheet and $\varepsilon < 0$ corresponds to shrinking sheet.

Following Mukhopadhyay and Andersson [46] we take $A = \sigma\sqrt{\nu/c}$ and $B = (\nu/c)\delta$ with $\sigma > 0$ being the first velocity slip and $\delta < 0$ is the second velocity slip parameters (see [7]).

The quantities of interest can be introduced as

$$C_f = \frac{\tau_w}{\rho U^2}, \quad \mathrm{Nu}_x = \frac{xq_w}{k(T_w - T_\infty)}, \quad \mathrm{Sh} = \frac{xq_m}{D_B(\phi_w - \phi_\infty)}, \tag{13}$$

where τ_w is the wall shear stress, q_w is the wall heat flux and q_m is the wall mass flux are given by

$$\tau_w = \mu\left(\frac{\partial u}{\partial y}\right)_{y=0}, \quad q_w = -k\left(\frac{\partial T}{\partial y}\right)_{y=0}, \quad q_m = -D_B\left(\frac{\partial \phi}{\partial y}\right)_{y=0}. \tag{14}$$

Using similarity transformation (7), we obtain

$$\begin{gathered} \mathrm{Re}_x^{1/2} C_f = f''(0), \\ \mathrm{Re}_x^{-1/2}\mathrm{Nu}_x = -\theta'(0), \\ \mathrm{Re}_x^{-1/2}\mathrm{Sh}_x = -\beta'(0), \end{gathered} \tag{15}$$

where $\mathrm{Re}_x = cx^2/\nu$ is the local Reynolds number (see Venkataramanaiah et al. [47]).

4. Stability flow

Rosca and Pop [10] and Weidman et al. [24] have shown that the lower branch solutions are unstable (not physically realizable), while the upper branch solutions are stable (physically realizable). We test these features by considering the unsteady form of Eqs. (3)–(5). Thus, we introduce the new dimensionless time variable τ,

$$\begin{gathered} u = cx\frac{\partial f}{\partial \eta}(\eta,\tau), \quad v = -\sqrt{c\nu}f(\eta,\tau), \quad \theta(\eta,\tau) = \frac{T - T_\infty}{T_w - T_\infty}, \\ \beta(\eta,\tau) = \frac{\phi - \phi_\infty}{\phi_w - \phi_\infty}, \quad \eta = y\sqrt{\frac{c}{\nu}}, \quad \tau = ct. \end{gathered} \tag{16}$$

The use of τ is associated with an initial value problem and is consistent with the question of which solution will be obtained in practice (physically realizable). Then the unsteady Eqs. (3)–(5) can be written as

$$\frac{\partial^3 f}{\partial \eta^3} + f\frac{\partial^2 f}{\partial \eta^2} - \left(\frac{\partial f}{\partial \eta}\right)^2 - \frac{\partial^2 f}{\partial \eta \partial \tau} = 0, \tag{17}$$

$$\frac{1}{\mathrm{Pr}}\frac{\partial^2 \theta}{\partial \eta^2} + f\frac{\partial \theta}{\partial \eta} + \mathrm{Nb}\,\frac{\partial \theta}{\partial \eta}\frac{\partial \beta}{\partial \eta} + \mathrm{Nt}\left(\frac{\partial \theta}{\partial \eta}\right)^2 - \frac{\partial \theta}{\partial \tau} = 0, \tag{18}$$

$$\frac{\partial^2 \beta}{\partial \eta^2} + \mathrm{Le} f\frac{\partial \beta}{\partial \eta} + \frac{\mathrm{Nt}}{\mathrm{Nb}}\frac{\partial^2 \theta}{\partial \eta^2} - \mathrm{Le}\,\frac{\partial \beta}{\partial \tau} = 0, \tag{19}$$

subjected to the boundary conditions

$$\begin{aligned}
&f(0,\tau) = s, \quad \frac{\partial f}{\partial \eta}(0,\tau) = \varepsilon + \sigma\frac{\partial^2 f}{\partial \eta^2} + \delta\frac{\partial^3 f}{\partial \eta^3},\\
&\frac{\partial \theta}{\partial \eta}(0,\tau) = \mathrm{Bi}\,(\theta(0,\tau) - 1), \quad \mathrm{Nb}\,\frac{\partial \beta}{\partial \eta}(0,\tau) + \mathrm{Nt}\,\frac{\partial \theta}{\partial \eta}(0,\tau) = 0,\\
&\frac{\partial f}{\partial \eta}(\infty,\tau) \to 0, \quad \theta(\infty,\tau) \to 0, \quad \beta(\infty,\tau) \to 0.
\end{aligned} \tag{20}$$

To test the stability of the steady flow solution $f(\eta) = f_0(\eta)$, $\theta(\eta) = \theta_0(\eta)$, and $\beta(\eta) = \beta_0(\eta)$ satisfying the boundary value problem (8)–(11), we write

$$\begin{aligned}
f(\eta,\tau) &= f_0(\eta) + e^{-\gamma\tau}F(\eta),\\
\theta(\eta,\tau) &= \theta_0(\eta) + e^{-\gamma\tau}G(\eta),\\
\beta(\eta,\tau) &= \beta_0(\eta) + e^{-\gamma\tau}H(\eta),
\end{aligned} \tag{21}$$

where γ is an unknown eigenvalue, $F(\eta)$, $G(\eta)$ and $H(\eta)$ are small relative to $f_0(\eta)$, $\theta_0(\eta)$ and $\beta_0(\eta)$. Solutions of the eigenvalue problem (17)–(19) give an infinite set of eigenvalues $\gamma_1 < \gamma_2 < \gamma_3 < \ldots$; if γ_1 is negative, there is an initial growth of disturbances and the flow is unstable but when γ_1 is positive, there is an initial decay and the flow is stable. Introducing (21) into (17)–(20), we get the following linearized problem

$$F_0''' + f_0F_0'' + f_0''F_0 - 2f_0'F_0' + \gamma F_0' = 0, \tag{22}$$

$$\frac{1}{Pr}G_0'' + f_0G_0' + F_0\theta_0' + \mathrm{Nb}\,\beta_0'G_0' + \mathrm{Nb}\,\theta_0'H_0' + 2\mathrm{Nt}\,\theta_0'G_0' + \gamma G_0 = 0, \tag{23}$$

$$H_0'' + \mathrm{Le}\,f_0H_0' + \mathrm{Le}\,F_0\beta_0' + \frac{\mathrm{Nt}}{\mathrm{Nb}}G_0'' + \mathrm{Le}\,\gamma H_0 = 0, \tag{24}$$

along with the boundary conditions

$$\begin{aligned}
&F_0(0) = 0, \quad F_0'(0) = \sigma F_0''(0) + \delta F_0'''(0),\\
&G_0'(0) = \mathrm{Bi}\,G_0(0), \quad \mathrm{Nb}\,H_0'(0) + \mathrm{Nt}\,G_0'(0) = 0,\\
&F_0'(\infty) \to 0, \quad G_0(\infty) \to 0, \quad H_0(\infty) \to 0.
\end{aligned} \tag{25}$$

It should be stated that for particular values σ, δ, Bi, Nb, Nt and Le the stability of the corresponding steady flow solutions $f_0(\eta)$, $\theta_0(\eta)$ and $\phi_0(\eta)$ are determined by the smallest eigenvalue γ. As it has been suggested by Harris et al. [48], the range of possible eigenvalues can be determined by relaxing a boundary condition on $F_0(\eta)$, $G_0(\eta)$ and $H_0(\eta)$. For the present problem, we relax the condition that $F_0'(\eta) \to 0$ as $\eta \to \infty$ for a fixed value of σ, δ, Bi, Nb, Nt and Le we solve the system (21)–(25) along with new boundary conditions $F_0'' = 1$.

5. Result and discussion

The partial differential equations PDEs (3)–(5) are transformed into nonlinear differential equations ODEs (8)–(10) using appropriate similarity variables (7). The order of ODEs is reduced to the first order systems before being applied into bvp4c function in Matlab software to obtain the numerical results which are the missing values of $f''(0)$, $-\theta'(0)$ and $-\beta'(0)$. The numerical results obtain are considered correct if the profiles (velocity, temperature and nanoparticle concentration) fulfill the boundary conditions (11) asymptotically.

Figures 2–5 represent the skin friction coefficient and heat transfer coefficient at stretching/shrinking surface for some values of the first and the second order slip, σ and δ respectively. The dual solutions obtained from all positive values (stretching case) up to critical value (shrinking case), ε_c. Beyond this value of ε_c there are no solutions occur because of no boundary layer separation. As we can see the skin friction coefficient and heat transfer rate are increasing as we increased the values σ and $|\delta|$. When we increased the values of $|\delta|$ (σ is absent), then the range of solution occurs is wider compared to when we increased the values of σ (δ is absent). More, the presence of the second order slip parameter δ will drag the boundary layer separation and hence the range of solution is much wider than if the first order slip σ is presented (see Figures 3–4). The heat loss from the plate becomes more quickly with the presence of the second order slip δ. Plus, the increasing values of the second order velocity slip $|\delta|$ will accelerate the heat transfer rate from the surface.

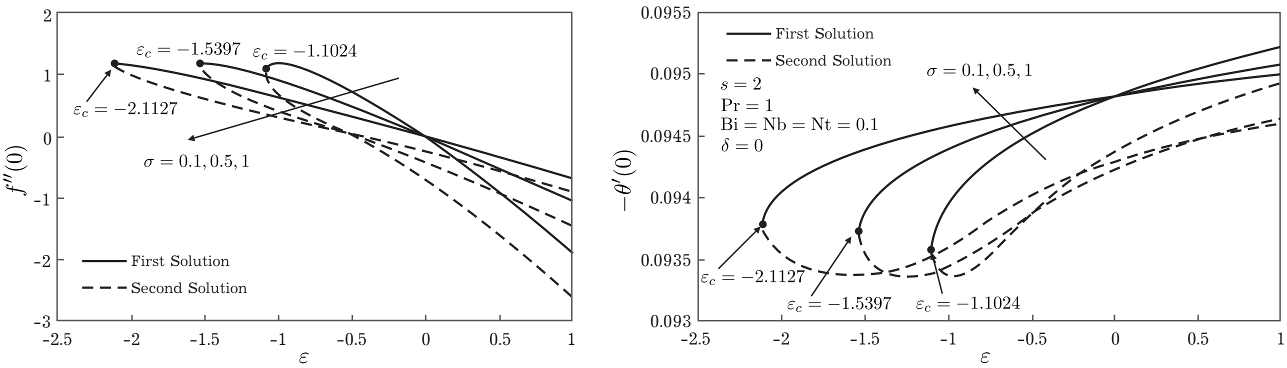

Fig. 2. Skin friction coefficient $f''(0)$ and heat transfer coefficient $-\theta'(0)$ vs ε for various values of σ and δ.

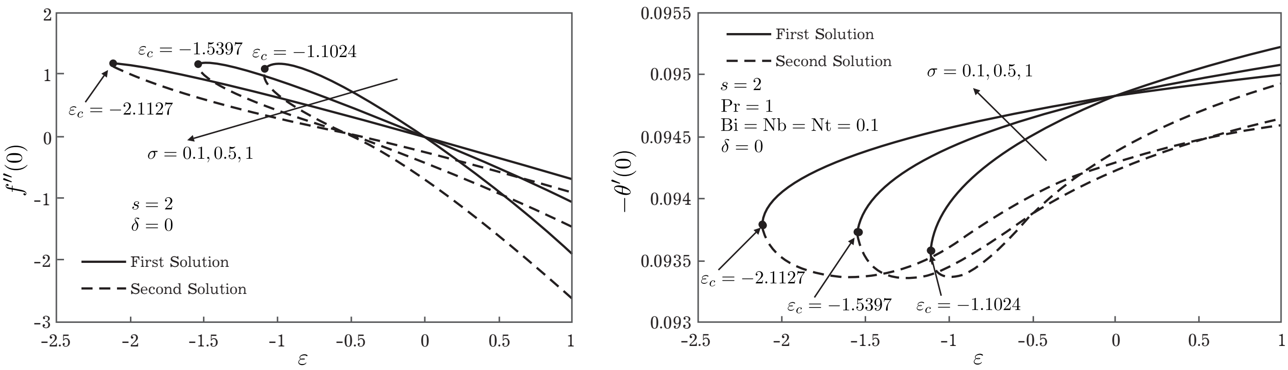

Fig. 3. Skin friction coefficient $f''(0)$ and heat transfer coefficient $-\theta'(0)$ vs ε for various values of σ.

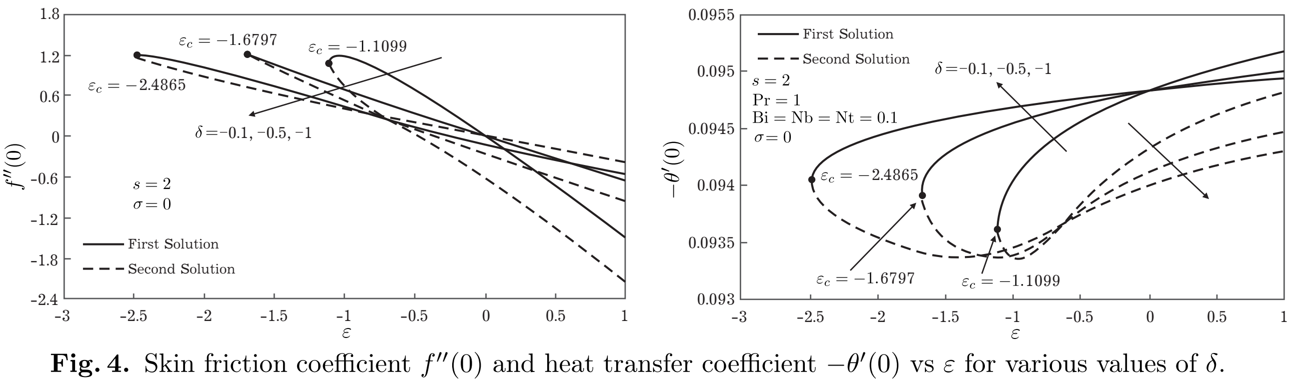

Fig. 4. Skin friction coefficient $f''(0)$ and heat transfer coefficient $-\theta'(0)$ vs ε for various values of δ.

Figure 5 shows the heat transfer coefficient for various values of Biot number, Bi. The higher value of Bi caused the stronger convection to occur and hence the heat transfers more quickly. Therefore, heat transfer increased as we increased the values of Bi.

Figure 6 physically shows the temperature profiles for the different values of Le. Figures 2–5 show that two (dual) solutions are obtained which are available in all range of the stretching/shrinking parameter ε and hence temperature profile in Figure 6 supported the existence of the dual solutions. On the other hand, we can see that the boundary layer thickness for the second solution is always thicker than the first solution.

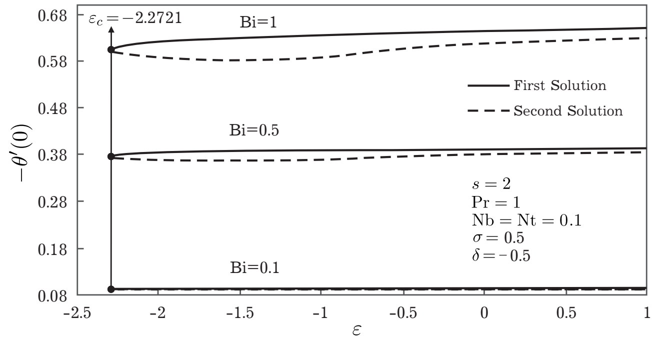

Fig. 5. Heat transfer coefficient $-\theta'(0)$ vs ε for various values of Bi.

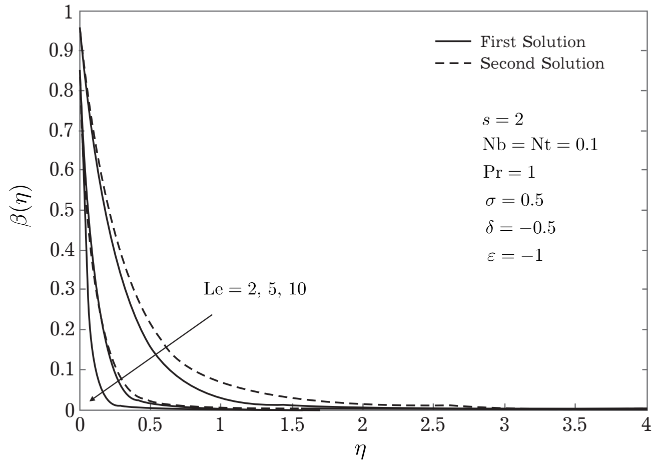

Fig. 6. Concentration profile $\beta(\eta)$ for various values of Le.

We perform a stability analysis to verify that the first solution is stable and physically relevant while the second solution acts in opposite way. The system of linear eigenvalue problems (22)–(24) along with the new boundary condition (25) is applied into the bvp4c to identify the values of the smallest eigenvalues γ. Only the certain range of involving dual solutions is chosen to test the stability analysis. We found that (see Table 1), the first solution (upper branch) is in stable state (positive value) while the second solution (lower branch) is unstable (negative value). From Table 1 we can say that as ε is approaching ε_c, the eigenvalues γ is approaching 0. The stable state is corresponding to the physically relevant because there is an initial decay on the flow whereas the second solution is unstable and defined as not physically relevant solution since there exist an initial growth of disturbance in the flow system.

Table 1. Smallest eigenvalues γ for selected values of ε with different σ and δ.

σ	δ	ε	First solution	Second solution
0	0	-1.0	0.0130	-0.0130
		-0.95	0.2703	-0.2385
		-0.8	0.5302	-0.4020
		-0.5	0.8006	-0.4848
		-0.3	1.2114	-0.5136
0.5	-0.5	-2.27	0.0420	-0.0418
		-2.2	0.2518	-0.2410
		-2.0	0.4818	-0.4394
		-1.5	0.7596	-0.6201
		-1.0	0.9073	-0.6276
1	-1	-3.66	0.0554	-0.0550
		-3.6	0.1873	-0.1828
		-3.0	0.5792	-0.5296
		-2.5	0.9762	-0.6426
		-2.0	1.0617	-0.6891

6. Conclusion

The steady boundary layer flow of a nanofluid past a stretching/shrinking plate in a uniform free stream in the presence of mass suction, thermal convective and the second order slip flow model introduced by Wu [6] is numerically studied. The boundary layer equations in form of partial differential equations (PDEs) are converted into ordinary differential equations (ODEs) using appropriate similarity variables before being solved using bvp4c function. The results reveal that

— dual solutions occurred for the skin friction coefficient, heat transfer rate and also mass transfer rate in all range of solution ε (stretching/shrinking parameter);
— the skin friction coefficient and heat transfer rate at the surface increase as the first and the second order slip parameter (σ and $|\delta|$) increases. The range of solution for the second order slip δ (the first order slip σ is absent) is much wider compare to when the first order slip parameter σ is considered;
— the presence of slip parameters causes to expand the range of the solutions;
— as Biot number Bi increases, the heat transfer is also increasing;
— smallest value of Brownian parameter Nb is sufficient enough to increase the mass transfer at the surface;
— higher thermophoresis parameter Nt will lead to increase the mass transfer rate at the surface;
— the first solution is linearly stable and physically relevant, while the second solution is linearly unstable and not physically relevant.

Acknowledgement

We would like to express appreciation to grant USIM/WUZI/FEM/ANTARABANGSA/40323 (Code: P2-6-244-40323-LUAR-WUZI-FEM) from University Sains Islam Malaysia.

[1] Shidlovskiy V. P. Introduction to The Dynamics of Rarefied Gas. American Elsevier Publishing Company Inc., New York (1967).

[2] Yoshimura A., Prud'homme R. K. Wall Slip Corrections for Couette and Parallel Disc Viscometers. Journal of Rheology. **32** (1), 53–67 (1988).

[3] Sharma I., Ishak A. Second Order Sslip Flow of Cu-water Nanofluid over a Stretching Sheet with Heat Transfer. WSEAS Trans. On Fluid Mech. **9**, 26–33 (2014).

[4] Japili N., Rosali H., Bachok N. MHD stagnation point flow over a stretching or shrinking sheet in a porous medium with velocity slip. Mathematical Modeling and Computing. **9** (4), 825–832 (2022).

[5] Alias N. S., Hafidzuddin M. E. H. Effect of suction and MHD induced Navier slip flow due to a non-linear stretching/shrinking sheet. Mathematical Modeling and Computing. **9** (1), 83–91 (2022).

[6] Wu L. A slip Model for Rarefied Gas Flows at Arbitrary Knudsen Number. Applied Physics Letters. **93** (25), 253103 (2008).

[7] Fang T., Yao S., Zhang J., Aziz A. Viscous Flow over a Shrinking Sheet with a Second-Order Slip Flow Model. Communications in Nonlinear Science and Numerical Simulation. **15** (7), 1831–1842 (2010).

[8] Fang T., Aziz A. Viscous Flow with Second-Order Slip Velocity over a Stretching Sheet. Zeitschrift für Naturforschung A. **65** (12), 1087–1092 (2010).

[9] Nandeppanavar M. M., Vajravelu K., Abel M. S., Siddalingappa M. N. Second Order Slip Flow and Heat Transfer over a Stretching Sheet with Nonlinear Navier Boundary Condition. International Journal of Thermal Sciences. **58**, 143–150 (2012).

[10] Roşca A. V., Pop I. Flow and Heat Transfer over a Vertical Permeable Stretching/Shrinking Sheet with a Second Order Slip. International Journal of Heat and Mass Transfer. **60**, 355–364 (2013).

[11] Singh G., Chamkha A. J. Dual Solutions for Second-Order Slip Flow and Heat Transfer on a Vertical Permeable Shrinking Sheet. Ain Shams Engineering Journal. **4** (4), 911–917 (2013).

[12] Alam M. S., Haque M. M., Uddin M. J. Convective Flow of Nanofluid along a Permeable Stretching/Shrinking Wedge with Second Order Slip using Buongiorno's Mathematical Model. International Journal of Advances in Applied Mathematics and Mechanics. **3** (3), 79–91 (2016).

[13] Buongiorno J. Convective Transport in Nanofluids. ASME Journal of Heat and Mass Transfer. **128** (3), 240–250 (2006).

[14] Mabood F., Shafiq A., Hayat T., Abelman S. Radiation Effects on Stagnation Point Flow with Melting Heat Transfer and Second Order Slip. Results of Physics. **7**, 31–42 (2017).

[15] Narayana K. L., Gangadhar K. Second Order Slip Flow of a MHD Micropolar Fluid over an Unsteady Stretching Surface. Advances in Applied Science Research. **6** (8), 224–241 (2015).

[16] Mabood F., Das K. Melting heat transfer on hydromagnetic flow of a nanofluid over a stretching sheet with radiation and second-order slip. The European Physical Journal Plus. **131**, 3 (2016).

[17] Wu L. Mass transfer induced slip effect on viscous gas flows above a shrinking/stretching sheet. International Journal of Heat and Mass Transfer. **93**, 17–22 (2016).

[18] Ibrahim W. MHD boundary layer flow and heat transfer of micropolar fluid past a stretching sheet with second order slip. Journal of the Brazilian Society of Mechanical Sciences and Engineering. **39**, 791–799 (2017).

[19] Kumar K. A., Sugunamma V., Sandeep N., Mustafa M. T. Simultaneous solutions for first order and second order slips on micropolar fluid flow across a convective surface in the presence of Lorentz force and variable heat source/sink. Scientific Reports. **9**, 14706 (2019).

[20] Salleh S. N. A., Bachok N., Ali F. M., Arifin N. M. Analysis of heat and mass transfer for second-order slip flow on a thin needle using a two-phase nanofluid model. Symmetry. **12** (7), 1176 (2020).

[21] Bakar S. A., Arifin N. M., Bachok N., Ali F. M. Hybrid nanofluid flow in a porous medium with second-order velocity slip, suction and heat absorption. Malaysian Journal of Mathematical Sciences. **16** (2), 257–272 (2022).

[22] Jauhri S., Mishra U. Numerical investigation of MHD nanofluid considering second-order velocity slip effect over a stretching sheet in porous media. Journal of Integrated Science and Technology. **11** (2), 478 (2023).

[23] Merkin J. H. On dual solutions occurring in mixed convection in a porous medium. Journal of Engineering Mathematics. **20**, 171–179 (1985).

[24] Weidman P. D., Kubitschek D. G., Davis A. M. J. The effect of transpiration on self-similar boundary layer flow over moving surfaces. International Journal of Engineering Science. **44** (11–12), 730–737 (2006).

[25] Merill K., Beauchesne M., Previte J., Paullet J., Weidman P. Final steady flow near a stagnation point on a vertical surface in a porous medium. International Journal of Heat and Mass Transfer. **49** (23–24), 4681–4686 (2006).

[26] Ishak A. Flow and Heat Transfer over a Shrinking Sheet: A Stability Analysis. International Science Index, Mathematical and Computational Sciences. **8** (5), 902–906 (2014).

[27] Hafidzuddin E. H., Nazar R., Arifin N. M., Pop I. Stability Analysis of Unsteady Three-Dimensional Viscous Flow over a Permeable Stretching/Shrinking Surface. Journal of Quality Measurement and Analysis. **11** (1), 19–31 (2015).

[28] Nazar R., Noor A., Jafar K., Pop I. Stability Analysis of Three-Dimensional Flow and Heat Transfer over a Permeable Shrinking Surface in a Cu-water Nanofluid. International Science Index, Mathematical and Computational Sciences. **8** (5), 782–788 (2014).

[29] Noor A., Nazar R., Jafar K. Stability Analysis of Stagnation-Point Flow Past a Shrinking Sheet in a Nanofluid. Journal of Quality Measurement and Analysis. **10** (2), 51–63 (2014).

[30] Noor A., Nazar R., Jafar K., Pop I. Stability Analysis of Flow and Heat Transfer on a Permeable Moving Plate in a Co-Flowing Nanofluid. AIP Conference Proceedings. **1614** (1), 898–905 (2014).

[31] Yasin M. H. M., Ishak A., Pop I. MHD Stagnation-Point Flow and Heat Transfer with Effects of Viscous Dissipation, Joule Heating and Partial Velocity Slip. Scientific Reports. **5**, 17848 (2015).

[32] Jahan S., Sakidin H., Nazar R., Pop I. Boundary layer flow of nanofluid over a moving surface in a flowing fluid using revised model with stability analysis. International Journal of Mechanical Sciences. **131–132**, 1073–1081 (2017).

[33] Jahan S., Sakidin H., Nazar R., Pop I. Analysis of heat transfer in nanofluid past a convectively heated permeable stretching/shrinking sheet with regression and stability analysis. Results in Physics. **10**, 395–405 (2018).

[34] Mustafa I., Abbas Z., Arif A., Javed T., Ghaffari A. Stability analysis for multiple solutions of boundary layer flow towards a shrinking sheet: Analytical solution by using least square method. Physica A: Statistical Mechanics and its Applications. **540**, 123028 (2020).

[35] Rehman A., Abbas Z. Stability analysis of heat transfer in nanomaterial flow of boundary layer towards a shrinking surface: Hybrid nanofluid versus nanofluid. Alexandria Engineering Journal. **61** (12), 10757–10768 (2022).

[36] Rasool G., Wang X., Yashkun U., Lund L. A., Shahzad H. Numerical treatment of hybrid water based nanofluid flow with effect of dissipation and Joule heating over a shrinking surface: Stability analysis. Journal of Magnetism and Magnetic Materials. **571**, 170587 (2023).

[37] Aziz A. A similarity solution for laminar thermal boundary layer over a flat plate with a convective surface boundary condition. Communications in Nonlinear Science and Numerical Simulation. **14** (4), 1064–1068 (2009).

[38] Noghrehabadi A., Pourrajab R., Ghalambaz M. Flow and heat transfer of nanofluids over stretching sheet taking into account partial slip and thermal convective boundary conditions. Heat and Mass Transfer. **49**, 1357–1366 (2013).

[39] Rashad A. M, Chamkha A. J., Modather M. Mixed convection boundary-layer flow past a horizontal circular cylinder embedded in a porous medium filled with a nanofluid under convective boundary condition. Computers & Fluids. **86**, 380–388 (2013).

[40] Makinde O. D., Mabood F., Khan W. A., Tshehla M. S. MHD flow of a variable viscosity nanofluid over a radially stretching convective surface with radiative heat. Journal of Molecular Liquids. **219**, 624–630 (2016).

[41] Ramesh G. K, Kumar K. G., Gireesha B., Shehzad S. A., Abbasi F. M. Magnetohydrodynamic nanoliquid due to unsteady contracting cylinder with uniform heat generation/absorption and convective condition. Alexandria Engineering Journal. **57** (4), 3333–3340 (2018).

[42] Ahmed S. E., Mahdy A. Buongiorno's nanofluid model for mixed convection flow over a vertical porous wedge with convective boundary conditions. Journal of Porous Media. **23** (10), 1001–1014 (2020).

[43] Rana P., Srikantha N., Muhammad T., Gupta G. Computational study of three-dimensional flow and heat transfer of 25 nm Cu-H_2O nanoliquid with convective thermal condition and radiative heat flux using modified Buongiorno model. Case Studies in Thermal Engineering. **27**, 101340 (2021).

[44] Khan W. A., Pop I. Boundary Layer Flow of a Nanofluid Past a Stretching Sheet. International Journal of Heat and Mass Transfer. **53** (11–12), 2477–2483 (2010).

[45] Makinde O. D., Aziz A. Boundary Layer Flow of a Nanofluid Past a Stretching Sheet with a Convective Boundary Conditions. International Journal of Thermal Sciences. **50** (7), 1326–1332 (2011).

[46] Mukhopadhyay S., Andersson H. I. Effects of slip and heat transfer analysis of flow over an unsteady stretching surface. Heat and Mass Transfer. **45**, 1447–1452 (2009).

[47] Venkataramanaiah G., Sreedharbabu M., Lavanya M. Heat Generation/Absorption Effects on Magneto-Williamson Nanofluidflow with Heat and Mass Fluxes. International Journal of Engineering Development and Research. **4** (1), 384–398 (2016).

[48] Harris S. D., Ingham D. B., Pop I. Mixed Convection Boundary-Layer Flow Near the Stagnation Point on a Vertical Surface in a Porous Medium: Brinkman Model with Slip. Transport in Porous Media. **77**, 267–285 (2009).

Чисельне дослідження впливу ковзання та термічної конвекції на граничний шар нанорідини за поверхнею розтягування/стискання

Наджіб Н.[1], Бачок Н.[2,3], Раседі А. Ф. Н.[1], Салле С. Н. А.[4], Сухаймі В. Н. В.[1]

[1] *Факультет економіки та Муамалат, Університет Святого Ісламу Малайзії, Бандар Бару Нілай, 71800 Нілай, Негері-Сембілан, Малайзія*

[2] *Інститут математичних досліджень, кафедра математики і статистики природничого факультету, Університет Путра Малайзія, 43400 Серданг, Селангор, Малайзія*

[3] *Коледж обчислювальної техніки, інформатики та математики, Технологічний університет МАРА Кедах, Мербок 08400, Кедах, Малайзія*

Дослідження сфокусоване на стаціонарному потоці в граничному шарі, тепло- та масообміні, який проходить через лист, що розтягується/стискається та занурений у нанорідину, за наявності швидкості ковзання другого порядку та теплової конвекції на межі. Основні диференціальні рівняння в частинних похідних перетворюються на звичайні диференціальні рівняння шляхом застосування змінних подібності перед чисельним розв'язуванням за допомогою функції bvp4c у програмному забезпеченні Matlab. Результати для поверхневого тертя, теплоперенесення, а також коефіцієнта теплопровідності як залежності визначальних параметрів, таких як параметр ковзання першого порядку, параметр ковзання другого порядку, число Біо, параметр броунівського руху та параметр термоферозу, подано графічно та обговорено. Подвійні розв'язки існують у всьому діапазоні параметрів розтягування та стиснення. Тому аналізується стійкість та робиться висновок, що перший розв'язок є стійким і фізично актуальним, тоді як другий розв'язок навпаки.

Ключові слова: *аналіз стійкості; лист, що розтягується/стискається; нанорідина; подвійний розв'язок; тепломасообмін; теплоконвективний.*